

# Crystal Growth by Unidirectional Method - A Generalized View on the Crystalline Perfection of the Uni-Indexed, Bi-Indexed, and Tri-Indexed Plane Single Crystals

Sivakumar Aswathppa, Sahaya Jude Dhas Sathiyadhas, V. Muthuvel, Lidong Dai,\* and Martin Britto Dhas Sathiyadhas Amalapushpam\*

In this article of generalized view, a comparison of the long-range order crystalline perfection of crystals is made with respect to their planes grown by the unidirectional growth technique. Based on the obtained results, it is established that the uni-indexed grown crystals yield a high degree of crystalline perfection and to a certain extent the bi-indexed crystals, but tri-indexed crystals grow with higher lattice disorders. Herein, uni-indexed crystal means the crystal grown along a plane has only one integer out of the h, k, and l whereas the other values are zero [e.g., (100), (010), (001)]. Bi-indexed crystal means the crystal grown along a plane has integers for any two of the h, k, and l but the remaining value is zero [e.g., (110), (011), (101)]. Tri-indexed crystal means the crystal grown along the plane has integers for all the values of h, k, and l [e.g., (111)].

atoms and molecules suffer variations in their orientations and bonding arrangements due to external parameters such as pressure, temperature variations, irradiations, etc.<sup>[1–3]</sup> Hence, the growth of bulk crystals without any lattice disorder is highly crucial and challenging. In order to overcome this critical situation, a lot of crystal growers have paid significant effort over the last few decades and found several direction-controlled growth techniques such as seed-oriented undercooled melt growth,<sup>[4]</sup> Microtube-Czochralski,<sup>[5]</sup> Vertical Bridgman method,<sup>[6]</sup> and Sankaranarayanan–Ramasamy method (SR method)<sup>[7]</sup> to grow bulk size crystals with high-degree of crystalline perfection. Among the

above-mentioned techniques, the SR method is one of the most popular methods due to the unidirectional crystal growth, minimum defects in the growth period as well as high solute-crystal conversion efficiency and high growth rate, etc.<sup>[7]</sup>

As far of now, a number of crystal growers have grown crystals using the SR method with different orientations and harvested good quality optically transparent crystals of bulk size. Benzophenone (110) was the first crystal grown by the SR method<sup>[7]</sup> and from thereon, numerous researchers have reported their respective crystal growth findings and the functional properties of the grown crystals.<sup>[8–29]</sup> For example, Balamurugan et al. have reported the crystal growth of KDP by the SR method along the uni-indexed plane of (200) and obtained good crystalline perfection<sup>[8]</sup> that are also reflected in the crystals of L-alaninium p-toluenesulfonate (010),<sup>[9]</sup> Triglycine sulfate (001),<sup>[10]</sup> triglycine sulfate (010),<sup>[11]</sup> Sodium sulfanilate dehydrate (001),<sup>[12]</sup> Methyl 2-amino-5-bromobenzoate (001),<sup>[13]</sup> ammonium dihydrogen phosphate (200),<sup>[14]</sup> benzophenone (100),<sup>[15]</sup> benzil (100),<sup>[16]</sup> nickel sulfate hexahydrate (004),<sup>[17]</sup> and ammonium dihydrogen phosphate (100),<sup>[18]</sup> D- $\pi$ -A type 2-amino-5-nitropyridinium dihydrogen phosphate (001),<sup>[19]</sup> Imidazolium L-Tartrate (010),<sup>[20]</sup> strontium bis (hydrogen L-malate) hexahydrate (010),<sup>[21]</sup> sulfamic acid (100),<sup>[22]</sup> L-alaninium p-toluenesulfonate (010),<sup>[23]</sup> and Triglycine calcium dibromide (001).<sup>[24]</sup> Comparatively low number of bi-indexed crystals were grown by the SR method and they are benzophenone (110)<sup>[7]</sup> 1,3,5-triphenylbenzene (011)<sup>[25]</sup> l-Glutamic acid hydrobromide,<sup>[26]</sup> 4-hydroxy l-proline (110)<sup>[27]</sup> t-stilbene,<sup>[28]</sup> ammonium dihydrogen phosphate (101),<sup>[29]</sup> and potassium

## 1. Introduction

“Crystals” that belong to the category of solid state of matter are characterized by long-range periodic order of the atoms or molecules in the micro-meter scale. Sometimes, these crystals experience lattice disorder in a non-periodic way wherein

S. Aswathppa, L. Dai  
Key Laboratory of High-Temperature and High-Pressure Study of the Earth's Interior, Institute of Geochemistry  
Chinese Academy of Sciences  
Guiyang, Guizhou 550081, China  
E-mail: dailidong@vip.gyig.ac.cn

S. J. D. Sathiyadhas  
Department of Physics  
Kings Engineering College  
Sriperumbudur, Chennai, Tamilnadu 602 117, India

V. Muthuvel  
Department of Physics, School of Foundation Science  
Kumaraguru College of Technology  
Coimbatore, Tamilnadu 641 049, India

M. B. D. Sathiyadhas Amalapushpam  
Shock Wave Research Laboratory, Department of Physics, Abdul Kalam Research Center  
Sacred Heart College  
Tirupattur, Vellore, Tamil Nadu 635 601, India  
E-mail: martinbritto@shctpt.edu

The ORCID identification number(s) for the author(s) of this article can be found under <https://doi.org/10.1002/crat.202300193>

DOI: 10.1002/crat.202300193

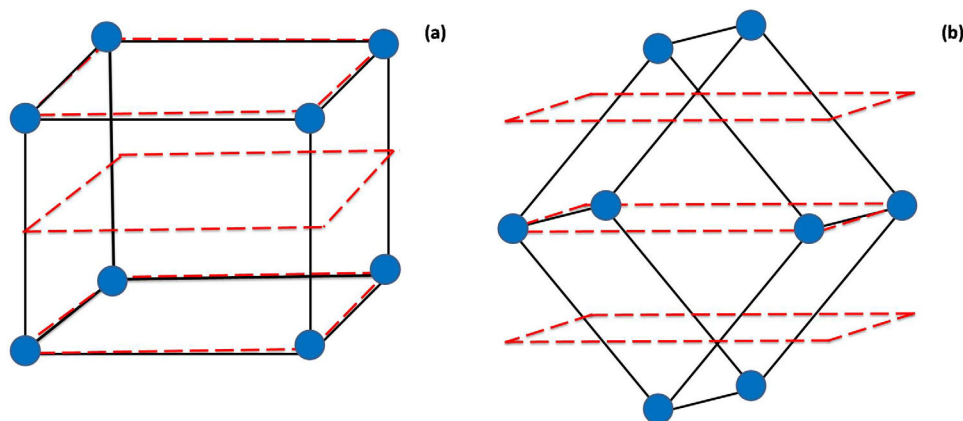


**Figure 1.** Schematic representation of planar arrangements a) uni-indexed crystal b) bi-indexed.

dihydrogen phosphate (101).<sup>[29]</sup> Tri-indexed plane crystal growth of ninhydrin (111)<sup>[30]</sup> by the SR method has been reported by Neelam Rani et al., and such kind of tri-indexed crystal growth by the SR method is rare and we have found, to date, only one report in this regard.

Note that, on the one hand, based on the above-mentioned reports, the uni-indexed planes such as (100), (010), and (001) crystals<sup>[8–24]</sup> have yielded good crystalline perfection and such results have been well-documented by the HRXRD analysis. On the other hand, in the case of bi-indexed plane crystals, crystalline perfection is comparably lower than that of uni-indexed crystals. Govindan et al., have reported the 1,3,5-triphenylbenzene single crystal and found a couple of satellite peaks that indicate the occurrence of the relative lattice disorder.<sup>[25]</sup> In addition to that, as per the ref [27] the bi-indexed crystal does not have any HRXRD or XRD results to confirm the degree of crystalline nature. More importantly, Sankaranarayanan et al., have grown (110) plane benzophenone crystals and observed one satellite peak along with a major broad diffraction curve wherein the full width at half maximum is 61 arc sec.<sup>[7]</sup> Senthil Pandian et al., have grown the same benzophenone crystal by the same technique along the (100) plane and found a very sharp diffraction peak in the HRXRD data and the full width at half maximum is 10 arc sec.<sup>[15]</sup> In addition to that, Neelam Rani et al., have reported ninhydrin crystal grown along the (111) plane employing the SR method and the results presented on the degree of crystalline perfection of the grown crystal remain to be not convincing.<sup>[29]</sup> Hence, the reliability of the degree of the crystalline nature of the grown crystal has to be counterchecked.

## 2. Results and Discussion

### 2.1. XRD Results

Based on the overall reported results, it is worthwhile to add a few more possible scientific facts about unidirectional crystal growth and the required knowledge for the selection of the apt plane for crystal growth to maintain a good degree of crystalline nature. A detailed understanding is highly helpful to the crystal growers in choosing the right plane for crystal growth such that highly long-range ordered crystals of bulk size can be grown for industrial

applications. Note that, the surface energy (step energy) values for a, b, and c-axes are different for a particular crystal that vary with respect to the material and its crystallographic phases.<sup>[32]</sup> Because of the anisotropy of the crystalline planes (especially bonding and planar density), the growth rates of the crystals are different from each other. While looking into a uni-indexed plane crystal, the surface energy of the crystal is uniform throughout such that uniform surface energy is required to build the long-range ordered units without any lattice frustration. Since there is no planar interface for the uni-indexed plane (i.e, isotropic surface free energy) normal growth of the crystal lattice in the same direction leads to a higher degree of crystalline nature (**Figure 1**). Therefore, while selecting a seed crystal it is essential to have uniform surface energy in such a way that high-quality unidirectional bulk size crystal can be grown and Figure 1 represents the arrangements of uni-indexed and bi-indexed planes in the respective crystal lattices.

On the other hand, bi-indexed and tri-indexed plane crystals have differences in surface energies and axial temperature gradient well within the crystal so that the staking of the repeated long-range order is reduced. Hence, the low surface energy plane grows faster than the higher surface energy planes so that bi-indexed seed crystals placed for the unidirectional growth encounter lattice disorder considerably compared to the uni-indexed plane crystals<sup>[7,25–28]</sup> while such disorder is more vigorous for the growing tri-indexed plane crystals.<sup>[29]</sup>

In the case of unidirectional growth imposed on bi-indexed and tri-indexed planes, the planar interfaces and planer density are linearly increased that leads to the resultant lattice disorder in the growing crystal. Note that generally, the bi-indexed and tri-indexed crystals' surfaces have more steps and kinks, etc than that of the uni-indexed plane crystal and the surfaces of such steps and kinks are highly dominant in the unidirectional crystal growth technique due to the anisotropic surface free energy in the crystal surface and the supplied incoming atoms and molecules cannot locate the lower energy point in the lattice to build a long-range ordered crystal. Note that, in the case of the unidirectional growth technique, the numbers of supplied atoms and molecules are the same across the growth surface that is controlled by the temperature gradient while the requirement of each axis is different in terms of the numbers of atoms to initiate the growth

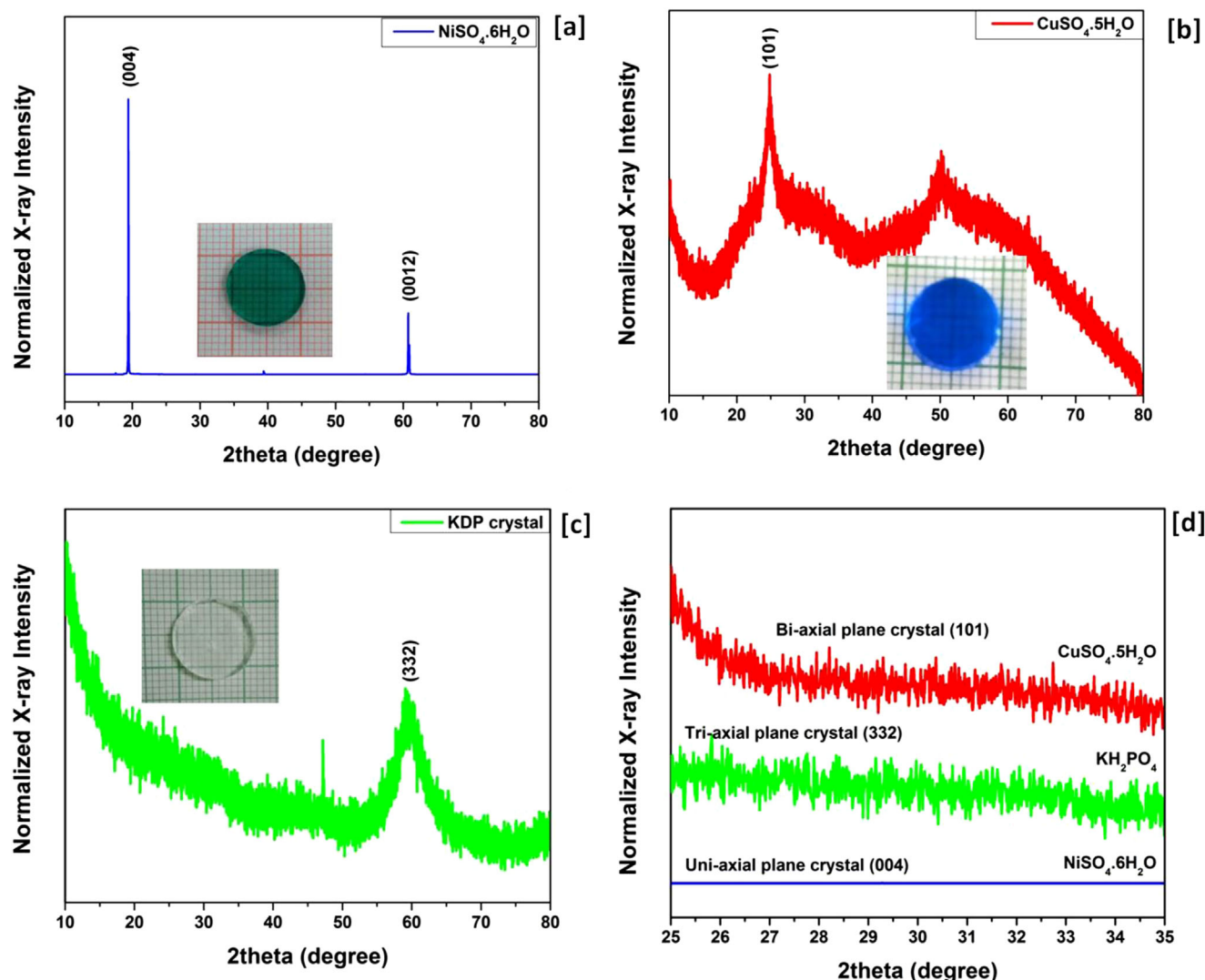


**Figure 2.** The XRD patterns of as grown crystals of uni-indexed, bi-indexed and tri-indexed planes a)  $\text{NiSO}_4 \cdot 6\text{H}_2\text{O}$  b)  $\text{CuSO}_4 \cdot 5\text{H}_2\text{O}$  c)  $\text{KH}_2\text{PO}_4$  d) XRD baseline width profile.

unit (as per the growth velocity of the axis). In the case of the unidirectional technique, crystals can grow easily in only one direction, i.e., without any lattice frustration as per the axial velocity of the crystal. But, while either the bi-indexed or the tri-indexed plane crystal is placed at the bottom of the ampoule, it is forced to grow along the respective axes simultaneously. Because of the existence of different axial velocities and non-uniform surface energy, all the directions cannot have lower energy points to build a perfect crystalline unit for the growing bi-indexed as well as tri-indexed crystals. The observed measurements of diffraction (XRD, HRXRD) of both bi-indexed and tri-indexed plane crystals have significant changes in terms of the degree of crystalline nature.<sup>[33–35]</sup> X-ray diffraction and X-ray topography techniques can act as simple and reliable methods to find direct evidence for the degree of crystalline nature of the grown crystals.<sup>[36–40]</sup> Here we have performed the X-ray diffraction techniques to justify the results. The crystallographic details of the grown crystals are such that  $\text{NiSO}_4 \cdot 6\text{H}_2\text{O}$  has crystallized in the tetragonal struc-

ture with the space group  $P4_12_12$  and the lattice dimensions are  $a = b = 6.785$ ,  $c = 18.279$  Å.<sup>[41]</sup>  $\text{CuSO}_4 \cdot 5\text{H}_2\text{O}$  belongs to the triclinic crystal system possessing the  $P-1$  space symmetry and the lattice dimensions are  $a = 6.106$ ,  $b = 10.656$ , and  $c = 5.969$  Å.<sup>[42]</sup> KDP crystal is crystallized in the tetragonal structure with the space group  $I4-2d$  and the lattice dimensions are  $a = 7.34$ ,  $b = 7.34$ , and  $c = 6.975$  Å.<sup>[43]</sup> As seen in **Figure 2a**, the nickel sulfate hexahydrate single crystal (uni-indexed plane – (004)) shows a strong and sharp diffraction peak without any baseline noise that indicates that the grown crystal has a higher degree of crystalline nature. We have utilized X-ray diffractometry (Rigaku-SmartLab X-ray Diffractometer, Japan) for the present investigation with  $\text{CuK}\alpha$  as the X-ray source ( $\lambda = 1.5407$  Å) of radiation and a 1D detector. The copper sulfate pentahydrate single crystal as in **Figure 2b** reflects the XRD pattern by which it is quite clear that the degree of crystalline nature is significantly affected due to the bi-indexed crystal growth in the SR method. **Figure 2c** exhibits the XRD pattern of as grown KDP crystal along the

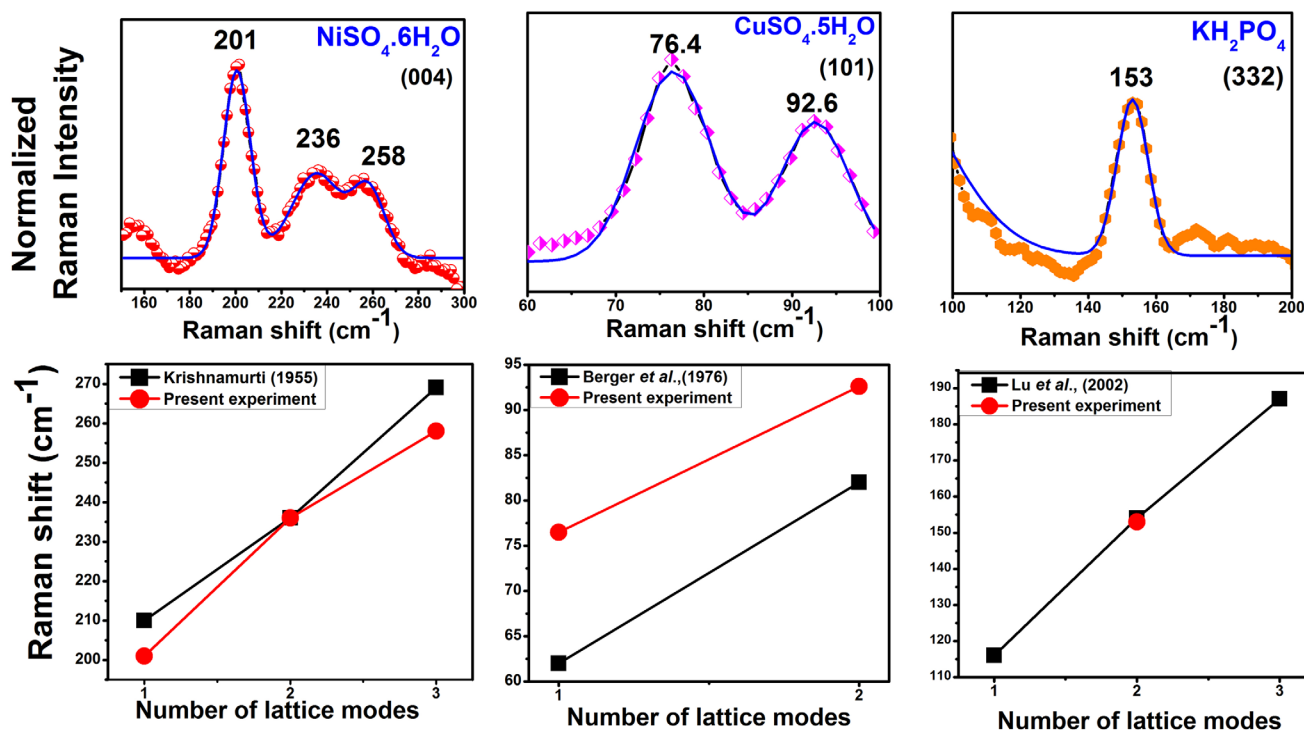


Figure 3. Lattice Raman modes of the grown uni-indexed, bi-indexed and tri-indexed planes of crystals.

tri-indexed plane in which the (332) plane diffraction peak has very low intensity and high full width at half maximum indicating the grown crystal's high structural disorder in comparison with the uni-indexed and bi-indexed plane crystals.<sup>[44]</sup>

Note that, the sharpness of the diffraction peak is reduced while increasing the order of planes, i.e., uni-indexed, bi-indexed and tri-indexed planes that indicate that the uni-indexed plane crystals are better candidates for the growth of crystals employing the unidirectional method to harvest bulk size of high-degree crystalline materials along a specific orientation. Apart from the diffraction peak characteristics, the baseline XRD profile of the above-motivated three single crystals is presented over the diffraction angle from 25–35° in Figure 2d wherein the tri-indexed plane crystal shows the highest degree of noise compared to the other two crystals. It indicates that the stacking units in the lattice may not be homogenous such that the lack of long-range period order, as well as high lattice strain, might cause the growing crystal to experience lattice frustration and end up in a lower crystalline symmetry material.

## 2.2. Lattice Raman Modes

Furthermore, in justifying the outcomes of the indented research, Raman spectroscopic results can provide more inroads into the local disorder of the crystal structure.<sup>[43–54]</sup> The recorded lattice modes Raman spectra of the grown crystals and the observed lattice Raman modes are presented in Figure 3. Note that, in the case of  $\text{NiSO}_4 \cdot 6\text{H}_2\text{O}$  for the (004) plane, the lattice Raman mode positions are observed at 210, 236, and 269 cm<sup>-1</sup> such that the observed Raman band positions are well-matched with the

previous reports.<sup>[45]</sup> Hence, it could be confirmed that the grown  $\text{NiSO}_4 \cdot 6\text{H}_2\text{O}$  crystal is free from the local disorder and hence possesses a high degree of crystalline nature. On the one hand, in the case of  $\text{CuSO}_4 \cdot 5\text{H}_2\text{O}$  crystal, a couple of lattice Raman bands at 76 and 92 cm<sup>-1</sup> are seen while on the other hand, such Raman bands should have appeared at 62 and 82 cm<sup>-1</sup> for the  $\text{CuSO}_4 \cdot 5\text{H}_2\text{O}$  crystal.<sup>[46]</sup> Such a significant difference in the lattice Raman band positions clearly shows the symmetry of the crystal that is slightly affected causing the loss of the degree of crystalline nature. Finally, the tri-indexed plane crystal (332) of the KDP sample's Raman spectra is shown in Figure 3 wherein only one lattice Raman mode is present at 153 cm<sup>-1</sup>. Note that the perfect tetragonal KDP crystal should have three lattice Raman modes at 116, 154, and 187 cm<sup>-1</sup>, respectively.<sup>[47]</sup> The absence of those two lattice Raman modes clearly shows that the perfect tetragonal unit cell was not formed during the crystal growth condition.<sup>[48]</sup>

In addition to that, to add color to the claims, the reported HRXRD plots of a few technologically important single crystals of uni-indexed and bi-indexed are presented in Figure 4 that have been grown by the SR method. As seen in Figure 4a,b, the benzophenone crystals of (100) and (110) planes showcase the full width at half maximum (FWHM) at 10 and 61 arc s, respectively.

Based on the obtained values, the bi-indexed plane crystal has a higher value of FWHM that clearly shows that the bi-indexed crystal has a lower degree of crystalline nature than that of uni-indexed plane crystal. Moreover, the same logic is noticed in the case of ADP and KDP crystals and the corresponding HRXRD profiles are shown in Figure 4c–f. In both ADP and KDP crystals grown by the SR method, the respective bi-indexed crystals have much higher FWHM values than that of the uni-indexed crystals that is due to the changes occurring in the axial

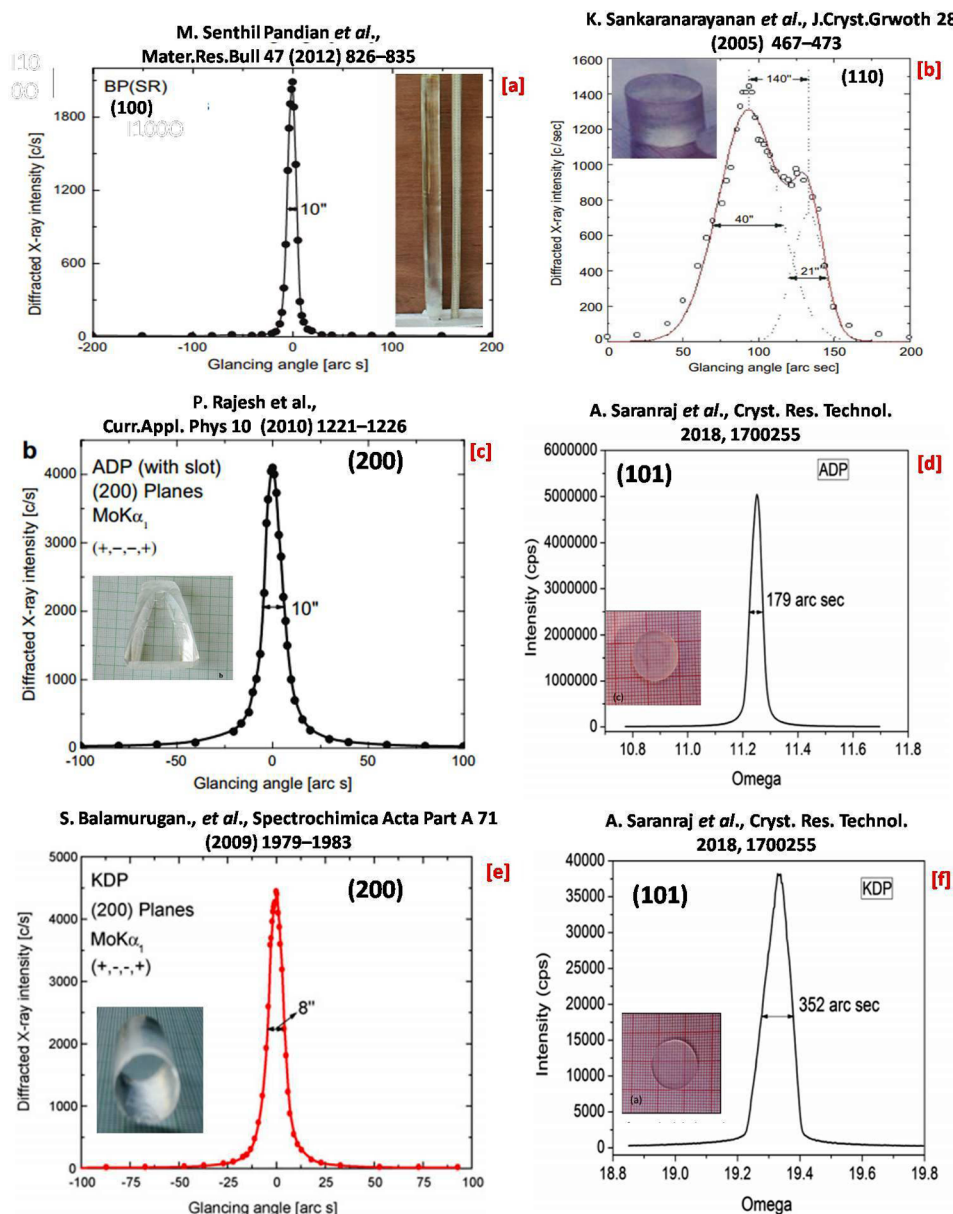


**Figure 4.** The HRXRD plots of uni-indexed and bi-indexed crystals of Benzophenone,<sup>[7,15]</sup> ADP,<sup>[14,29]</sup> and KDP crystals<sup>[8,29]</sup> wherein all the images are reprinted with permission.

temperature gradient while increasing the number of contributed axes during the crystal growth.<sup>[29]</sup> Furthermore, these changes enforce massive interface shear stress, radial shear stress, and axial shear stress<sup>[33–35]</sup> that leads to a poor crystalline nature compared to the uni-indexed crystals. For a better understanding of the above-mentioned HRXRD results, the comparative analysis of FWHM values for the uni-indexed and bi-indexed crystals is portrayed in Figure 5. Note that, as per the Figure 5 data points, the bi-indexed crystals have higher values of FWHM than that of the uni-indexed plane crystals.

In order to get more authentic information about the above-discussed results, we have grown uni-indexed and bi-indexed and tri-indexed planes of NiSO<sub>4</sub>·6H<sub>2</sub>O crystals by unidirectional tech-

nique and their respective recorded XRD patterns are presented in Figure 6. Based on the observed XRD results, it is authenticated that the degree of crystalline order is high for (004) plane and quite low for (1010) plane whereas a significant reduction is observed in the case of (4211) plane compared to the (004) plane. The poor crystalline nature of the (4211) plane may be due to the lack of long-range period order as well as high lattice strain which might have developed in the growing crystal leading to experience lattice frustration that could have ended up with a lower degree of crystalline nature.

In addition to that, from the provided diffraction angle from 25 to 45 degrees (Figure 1d), the diffraction baseline width is found to be linearly increased that clearly demonstrates that the degree

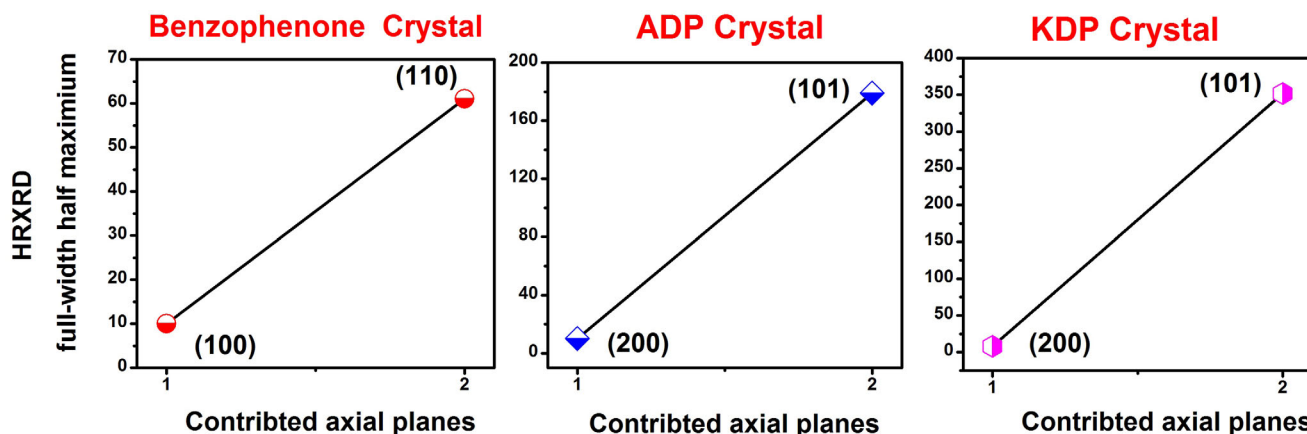


Figure 5. FWHM values of uni-indexed and bi-indexed crystals of Benzophenone,<sup>[7,15]</sup> ADP,<sup>[14,29]</sup> and KDP crystals.<sup>[8,29]</sup>

of lattice disorder increases for higher order indexes. Note that, in the case of  $\text{NiSO}_4 \cdot 6\text{H}_2\text{O}$  for the (004) plane, the lattice Raman mode positions are observed at 210, 236, and 269  $\text{cm}^{-1}$  such that the observed Raman band positions are found to be well-matched with the previous reports (Figure 7).<sup>[44]</sup> In the case of the (1010) plane, the dominant Raman mode is shifted toward the lower wavenumber while one lattice Raman mode has disappeared and this can be convincing evidence for the increase of local lattice disorder in the grown crystal.<sup>[48–55]</sup> More interestingly, in the case of the (4211) plane, the lattice Raman mode is shifted from 201 to 192  $\text{cm}^{-1}$  while here also one higher wavenumber lattice Raman mode has disappeared and such kind of significant changes

in the Raman lattice modes clearly show the formation of local lattice disorder in the case of the (4211) plane.<sup>[48–55]</sup>

The Differential Scanning Calorimetric (DSC) technique is well established to be one of the powerful tools to distinguish the crystalline and the amorphous states of the solid-state samples<sup>[56,57]</sup> such that the required DSC study is performed to reaffirm the degree of crystalline nature of the NSH sample with respect to their planes. Note that dehydration of water molecules is not dealt with for the NSH sample as more focus is given to the melting point of the DSC measurements that were performed using a DSC60 plus in the temperature range of 35 to 300 °C at a scanning rate of 5 °C  $\text{min}^{-1}$  in the nitrogen gas atmosphere. The

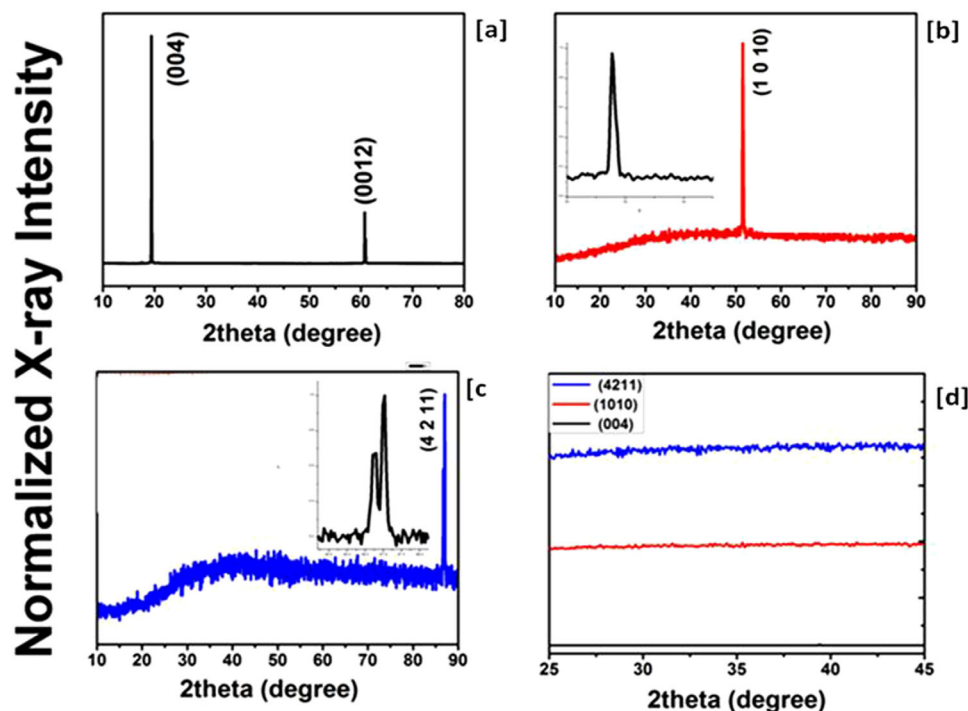


Figure 6. The XRD patterns of the as grown crystals of a) uni-indexed, b) bi-indexed, and c) tri-indexed planes of  $\text{NiSO}_4 \cdot 6\text{H}_2\text{O}$  d) zoomed-in version of the uni-indexed, bi-indexed, and tri-indexed planes to visualize the lattice frustration.

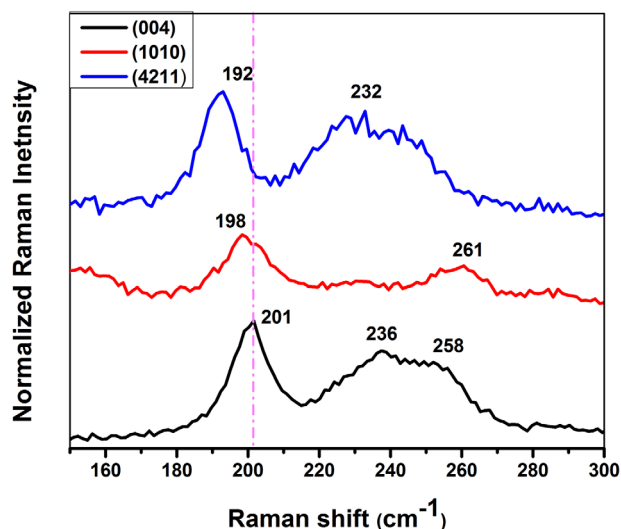


Figure 7. Lattice Raman spectra of the as grown crystals of uni-indexed, bi-indexed, and tri-indexed planes of  $\text{NiSO}_4 \cdot 6\text{H}_2\text{O}$ .

recorded DSC thermograms for the NSH samples are displayed in Figure 8.

The existing endothermic peak positions of the NHS sample are located for the (004) plane at 108.22, 140.19, 156.9, and 168.3 °C, respectively and for the bi-index at 108.22, 125.13, 140, 154.37, and 170.01 °C, respectively and for the tri-index at 110.75, 128.11, 129.51, 140.39, and 167.08 °C, respectively. The exact endothermic peak positions for these three crystal planes along with the literature reports are shown in Figure 9. It is very well known that, based on the heating rate, the number of endothermic peaks

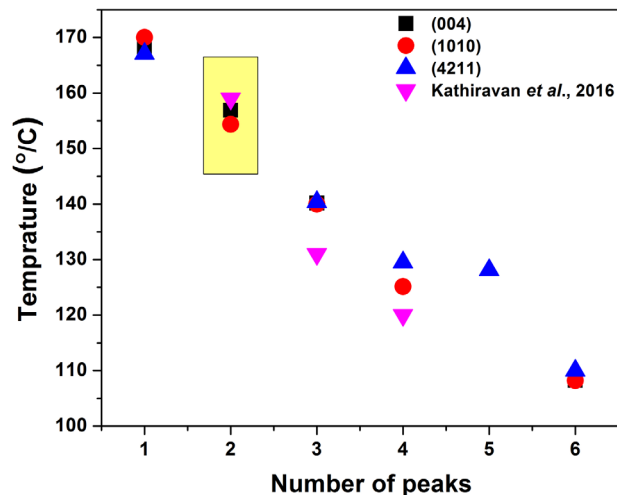


Figure 9. Number of endothermic peaks for the uni-indexed, bi-indexed, and tri-indexed planes of  $\text{NiSO}_4 \cdot 6\text{H}_2\text{O}$  crystals.

and their respective shapes may change.<sup>[58–60]</sup> Kathiravan et al., have reported three endothermic peaks at 120.45, 131.81, and 159 °C, respectively for the highly crystalline NSH samples at the heating rate of 10 °C min<sup>-1</sup>.<sup>[61]</sup> Among the three peaks, the endothermic peak at  $\approx 159$  °C is the most crucial one because it must have the highest intensity of the heat flow than the other endothermic peaks and similar results have been found for the uni-indexed crystal whereas slight changes are noticed for the bi-axial crystal such that a new endothermic peak is identified at 125.1 °C. The new endothermic peak generation clearly represents the local re-organization of atomic arrangements and the existing poor crystalline nature of the bi-indexed crystal. Similarly, the

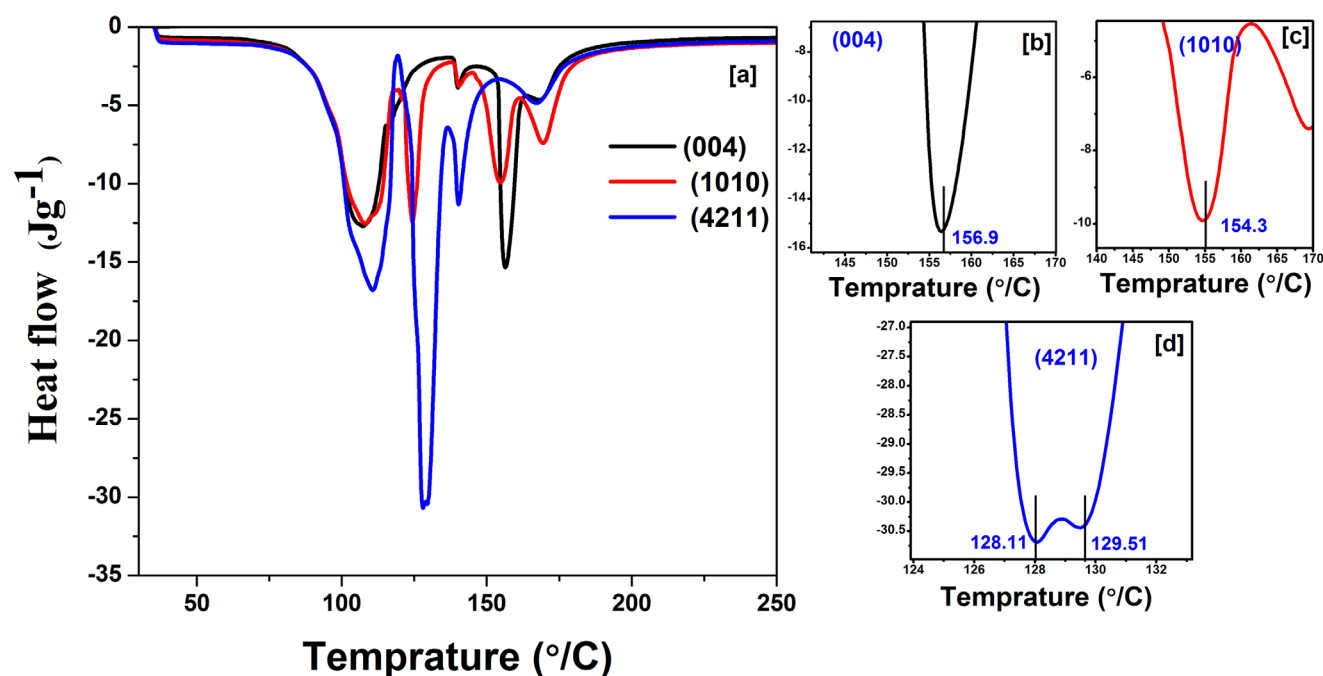


Figure 8. a) DSC thermograms of the as grown crystals of uni-indexed, bi-indexed, and tri-indexed planes of  $\text{NiSO}_4 \cdot 6\text{H}_2\text{O}$ . Zoomed-in portions of b) uni-indexed, c) bi-indexed, and d) tri-indexed planes of  $\text{NiSO}_4 \cdot 6\text{H}_2\text{O}$ .

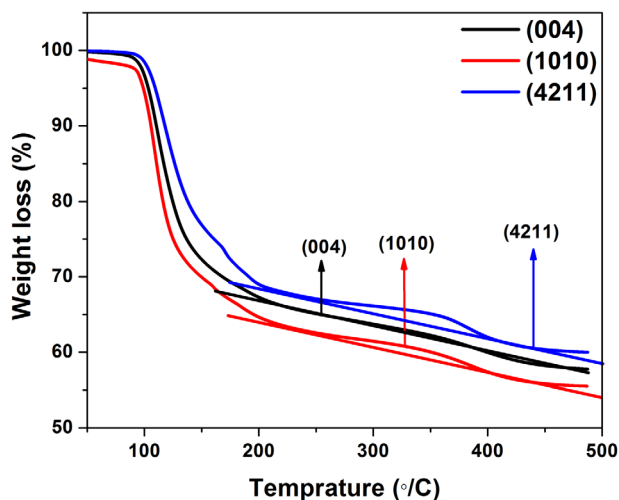


Figure 10. TGA plots of uni-indexed, bi-indexed, and tri-indexed planes of the as grown crystals of  $\text{NiSO}_4 \cdot 6\text{H}_2\text{O}$ .

corresponding peak has a very high intensity for the tri-indexed crystal and also found that the major endothermic peak at  $\approx 159^\circ\text{C}$  has disappeared that clearly authenticates that the degree of crystalline nature is poor compared to the bi-indexed

crystal. In addition to that, for better clarity on the degree of crystalline nature with respect to their planes, the zoomed-in portions of the high-intensity endothermic peaks are presented in Figure 8b–d for the uni-indexed, bi-indexed and tri-indexed planes of  $\text{NiSO}_4 \cdot 6\text{H}_2\text{O}$ . For the tri-indexed plane of the NSH sample, endothermic peak splitting could be noticed that is convincing proof for the poor crystalline nature.

In Figure 10, the TGA profiles of the uni-indexed, bi-indexed and tri-indexed planes of  $\text{NiSO}_4 \cdot 6\text{H}_2\text{O}$  crystals are presented. As seen in Figure 10, the weight loss tangent is uniform from 200 to  $480^\circ\text{C}$  for the uni-indexed NSH samples that is one of the strong supportive evidence for the higher degree of crystalline nature. The weight loss tangent over the same temperature region is significantly altered for the bi-indexed and tri-indexed planes of  $\text{NiSO}_4 \cdot 6\text{H}_2\text{O}$  crystals. Moreover, the tri-indexed plane samples' tangent area is comparatively high that clearly substantiates the highly disordered nature of the crystal.<sup>[62–65]</sup>

In addition to that, the observed XRD patterns of the uni-indexed, bi-indexed and tri-indexed plane crystals that have been grown by slow evaporation growth technique at ambient temperature are presented in Figure 11. As seen in Figure 11, all the uni-indexed, bi-indexed and tri-indexed plane crystals have good crystalline nature of long-range order.<sup>[66–69]</sup>

In the case of non-directional growth techniques (i.e., slow evaporation technique), all the available atoms/molecules can

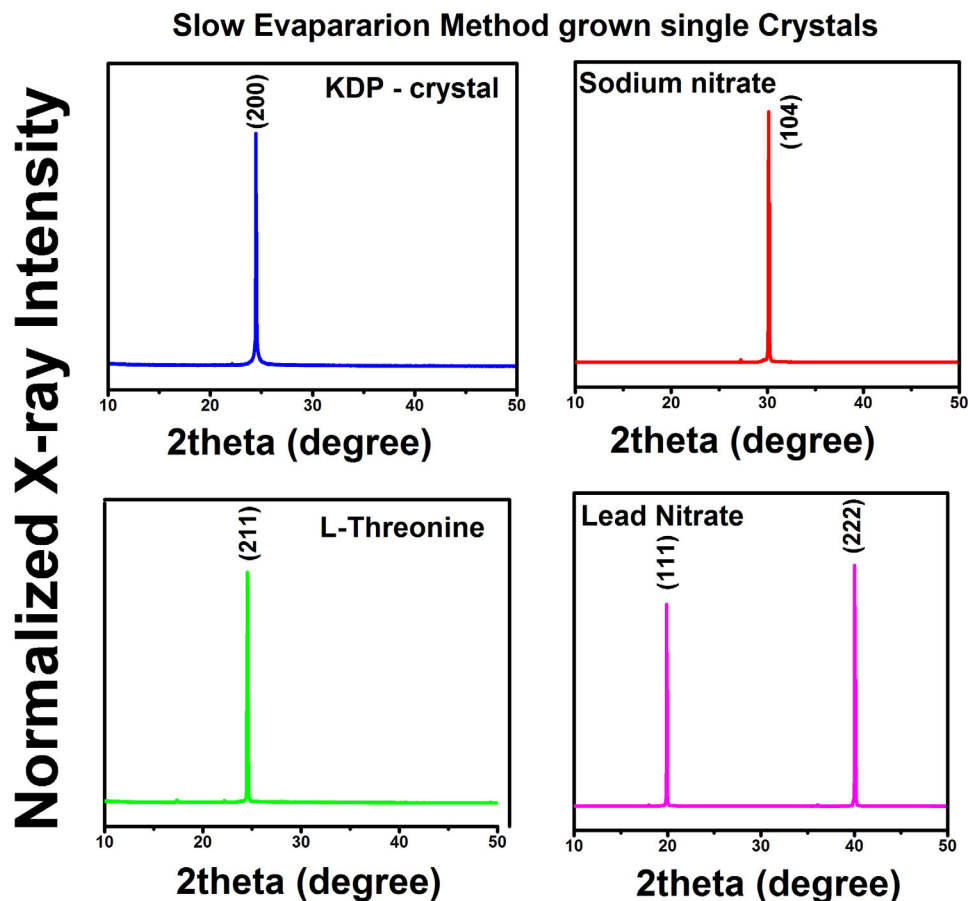


Figure 11. XRD patterns of as grown crystals employing the slow evaporation method.



find the low energy lattice points by themselves in the respective axis due to the time-dependent axial growth velocity of the crystal, and hence the growth is highly ordered. Also, in the case of the slow evaporation technique, though the numbers of available atoms for the uni-indexed, bi-indexed and tri-indexed planes are the same, each axis can have access to accommodate the required numbers of atoms to build the growth unit as per the growth of the axial velocity of the crystal structure with respect to time. Hence, even tri-indexed crystals can be grown with good crystalline nature compared to the crystals grown by unidirectional technique.

### 3. Conclusion

As a generalization of the investigations, we have presented the axial-dependent crystalline perfection of the SR method-grown single crystals such that the uni-indexed plane crystal is the best choice to grow a high degree of crystalline material compared to the bi-indexed and tri-indexed crystals. Literature reports also authenticate the findings of tri-indexed crystals possessing the higher lattice disorder because of the contribution of three different axial during the crystal growth such that the stacking of units may not be homogenous. Therefore, it is suggested that the uni-indexed planes of crystals such as (100), (010), and (001) are better and more suitable candidates for growing good quality crystals employing the SR method. On the other hand, the slow evaporation technique can be considered as an apt method to harvest tri-indexed crystals of a good crystalline nature.

### 4. Experimental Section

The unidirectional crystal growth processes were discussed in the group's previous publications<sup>[16–18,31]</sup> and the details of the crystal growth procedure are provided in the Supporting Information. The cut and polished single crystals of these materials measuring 1 mm thickness each were utilized for the present investigation, such that the uni-indexed plane crystal - NiSO<sub>4</sub>·6H<sub>2</sub>O (004), bi-indexed plane crystal- CuSO<sub>4</sub>·5H<sub>2</sub>O (101), and tri-indexed plane crystal- KH<sub>2</sub>PO<sub>4</sub> (332) were selected that were grown by the above-mentioned unidirectional crystal growth method.

### Supporting Information

Supporting Information is available from the Wiley Online Library or from the author.

### Acknowledgements

The authors thank the Abraham Panampara Research Fellowship and NSF of China (42072055). The authors thank Prof. P. Ramasamy and Dr. M. Senthil Pandian, SSN College of Engineering, Kalavakkam, Tamilnadu, India and Dr. A. Saranraj, Department of Physics, Government Arts and Science College for Women, Barugur, Krishnagiri, Tamilnadu, India for their fruitful discussions and suggestions.

### Conflict of Interest

The authors declare no conflict of interest.

### Data Availability Statement

The data that support the findings of this study are available from the corresponding author upon reasonable request.

### Keywords

degree of crystalline nature, directional solidification, growth from solutions, single crystal growth, X-ray diffraction

Received: June 29, 2023

Revised: September 9, 2023

Published online: October 15, 2023

- [1] A. Simonov, A. L. Goodwin, *Nat. Rev. Chem.* **2020**, *4*, 657.
- [2] H. Tong, P. Tan, N. Xu, *Sci. Rep.* **2015**, *5*, 15378.
- [3] S. Dagdale, V. Pahurkar, G. Muley, *Macromol. Symp.* **2016**, *362*, 139.
- [4] W. Wang, W. Huang, Y. Ma, J. Zhao, *J. Cryst. Growth* **2004**, *270*, 469.
- [5] K. Sankaranarayanan, P. Ramasamy, *J. Cryst. Growth* **1998**, *193*, 252.
- [6] M. Arivanandhan, K. Sankaranarayanan, K. Ramamoorthy, C. Sanjeeviraja, P. Ramasamy, *Cryst. Res. Technol.* **2004**, *39*, 692.
- [7] K. Sankaranarayanan, P. Ramasamy, *J. Cryst. Growth* **2005**, *280*, 467.
- [8] S. Balamurugan, P. Ramasamy, *Spectrochim. Acta A* **2009**, *71*, 1979.
- [9] V. Thayanithi, K. Rajesh, P. P. Kumar, *Mater. Res. Express* **2017**, *4*, 086201.
- [10] M. S. Pandian, N. Balamurugan, V. Ganesh, P. V. Raja Shekar, K. Kishan Rao, P. Ramasamy, *Mater. Lett.* **2008**, *62*, 3830.
- [11] M. S. Pandian, S. Verma, P. Karuppasamy, P. Ramasamy, V. S. Tiwari, A. K. Karnal, *J. Mater. Sci: Mater. Electron.* **2021**, *32*, 15778.
- [12] M. Senthil Pandian, P. Ramasamy, *Mater. Chem. Phys.* **2012**, *132*, 1019.
- [13] M. Parthasarathy, R. Gopalakrishnan, *J. Cryst. Growth* **2013**, *372*, 100.
- [14] P. Rajesh, P. Ramasamy, G. Bhagavannarayana, B. Kumar, *Curr. Appl. Phys.* **2010**, *10*, 1221.
- [15] M. Senthil Pandian, K. Boopathi, P. Ramasamy, G. Bhagavannarayana, *Mater. Res. Bull.* **2012**, *47*, 826.
- [16] A. Saranraj, J. Thirupathy, S. S. J. Dhas, M. Jose, G. Vinitha, S. A. Martin Britto Dhas, *Appl. Phys. B* **2018**, *124*, 97.
- [17] J. Thirupathy, S. Sahaya Jude Dhas, M. Jose, S. A. M. B. Dhas, *Mater. Res. Express* **2019**, *6*, 086206.
- [18] P. Rajesh, P. Ramasamy, G. Bhagavannarayana, B. Kumar, *Curr. Appl. Phys.* **2010**, *10*, 1221.
- [19] V. Sivasubramani, C. Anil Kumar, M. Venkatesh, A. Raja, G. Vinitha, M. S. Pandian, P. Ramasamy, *Cryst. Growth Des.* **2019**, *19*, 6873.
- [20] N. Elavarasu, S. Karuppasamy, S. Muralidharan, M. Anantharaja, R. Gopalakrishnan, *Opt. Mater.* **2015**, *46*, 141.
- [21] A. Senthil, P. Ramasamy, *J. Cryst. Growth* **2014**, *401*, 200.
- [22] M. Senthil Pandian, U. Charoen In, P. Ramasamy, P. Manyum, M. Lenin, N. Balamurugan, *J. Cryst. Growth* **2010**, *312*, 397.
- [23] V. Thayanithi, K. Rajesh, P. P. Kumar, *Mater. Res. Express* **2017**, *4*, 086201.
- [24] G. Babu Rao, P. Rajesh, P. Ramasamy, *J. Cryst. Growth* **2016**, *440*, 47.
- [25] V. Govindan, D. Joseph Daniel, H. J. Kim, K. Sankaranarayanan, *Mater. Chem. Phys.* **2019**, *223*, 183.
- [26] M. Senthilkumar, P. K. Singh, V. Singh, R. Sathyalakshmi, K. Pandiyan, R. K. Karn, *Phase Transitions* **2019**, *93*, 83.
- [27] L. Jayanthi, N. Prabavathi, V. Sivasubramani, M. Senthil Pandian, P. Ramasamy, S. A. Martin Britto Dhas, *J. Mater. Sci.: Mater. Electron.* **2017**, *28*, 15354.
- [28] V. Govindan, D. Joseph Daniel, H. J. Kim, K. Sankaranarayanan, *Dyes Pigm.* **2019**, *160*, 848.

- [29] A. Saranraj, A. S. Jenipriya, S. Sahaya Jude Dhas, M. Jose, S. A. Martin Britto Dhas, *Cryst. Res. Technol.* **2018**, *53*, 1700255.
- [30] N. Rani, N. Vijayan, B. Riscob, S. Karan Jat, A. Krishna, S. Das, G. Bhagavannarayana, B. Rath, M. A. Wahab, *CrystEngComm* **2013**, *15*, 2127.
- [31] J. Thirupathy, S. S. J. Dhas, S. A. Martin Britto Dhas, *J. Electron. Mater.* **2022**, *51*, 3132.
- [32] A. G. Stack, J. R. Rustad, J. J. Deyoreo, T. A. Land, W. H. Casey, *J. Phys. Chem. B* **2004**, *108*, 18284.
- [33] E. S. Jeong, *KSME J.* **1995**, *9*, 225.
- [34] M. A. Deij, J. H. Los, H. Meekes, E. Vlieg, *J. Appl. Crystallogr.* **2006**, *39*, 563.
- [35] W. Jo, N. M. Hwang, D. Y. Kim, *J. Korean Ceram. Soc.* **2006**, *43*, 728.
- [36] D. A. Zolotov, A. V. Buzmakov, V. E. Asadchikov, A. E. Voloshin, V. N. Shkurko, I. S. Smirnov, *Crystallogr. Rep.* **2011**, *56*, 393.
- [37] A. E. Voloshin, S. I. Kovalev, M. S. Lyasnikova, E. K. h. Mukhamedzhanov, M. M. Borisov, M. V. Koval'chuk, *Crystallogr. Rep.* **2012**, *57*, 670.
- [38] D. A. Romanov, I. A. Prokhorov, A. E. Voloshin, V. G. Kosushkin, A. P. Bolshakov, V. G. Ralchenko, *J. Surf. Investig.* **2020**, *14*, 1113.
- [39] A. Sivakumar, S. Sahaya Jude Dhas, S. Balachandrar, S. A. Martin Britto Dhas, *Z. Kristallogr.* **2019**, *234*, 557.
- [40] A. Sivakumar, P. E., S. Sahaya Jude Dhas, J. Kalyana Sundar, P. Sivaprakash, S. Arumugam, S. A. Martin Britto Dhas, *Z. Kristallogr.* **2020**, *235*, 193.
- [41] V. M. Masalov, A. A. Zhokhov, V. L. Manomenova, E. B. Rudneva, A. E. Voloshin, G. A. Emelchenko, *Crystallogr. Rep.* **2015**, *60*, 963.
- [42] V. L. Manomenova, M. N. Stepnova, V. V. Grebenev, E. B. Rudneva, A. E. Voloshin, *Crystallogr. Rep.* **2013**, *58*, 513.
- [43] H. A. R. Aliabad, M. Fathabadi, I. Ahmad, *Int. J. Quantum Chem.* **2013**, *113*, 865.
- [44] A. Sivakumar, S. Sahaya Jude Dhas, A. Saranraj, R. Sankar, R. S. Kumar, A. I. Almansour, I. Kim, S. A. Martin Britto Dhas, *Phys. B: Condens. Matter* **2022**, *644*, 414233.
- [45] D. Krishnamurti, *Proc. Ind. Acad. Sci.* **1955**, *42*, 77.
- [46] J. Berger, *J. Raman Spectrosc.* **1976**, *5*, 103.
- [47] G. W. Lu, X. Sun, *Cryst. Res. Technol.* **2002**, *37*, 93.
- [48] A. C. Ferrari, J. Robertson, *Phys. Rev. B* **2000**, *61*, 14095.
- [49] A. C. Ferrari, J. Robertson, *Phys. Rev. B* **2002**, *64*, 075414.
- [50] S. Chen, Z. Yao, H. Lv, E. Dong, X. Yang, R. Liu, B. Liu, *Phys. Chem. Chem. Phys.* **2018**, *20*, 26117.
- [51] K. Kamali, T. R. Ravindran, N. V. Chandra Shekar, K. K. Pandey, S. M. Sharma, *J. Solid State Chem.* **2015**, *221*, 285.
- [52] M. Maczka, K. Szyborska-Malek, G. D. e Sousa Pinheiro, P. T. Cavalcante Freire, A. Majchrowski, *J. Solid State Chem.* **2015**, *228*, 239.
- [53] C. Y. Xu, P. X. Zhang, L. Yan, *J. Raman Spectrosc.* **2001**, *32*, 862.
- [54] Y. Ren, H. Zhang, J. Zhang, X. Cheng, L. Jiang, Z. Chen, H. Dai, *J. Mol. Struct.* **2020**, *1210*, 127987.
- [55] A. Sivakumar, S. S. Jude Dhas, S. Chakraborty, R. S. Kumar, A. I. Almansour, N. Arumugam, S. A. M. B. Dhas, *J. Phys. Chem. C* **2022**, *126*, 3194.
- [56] A. Yazdani, G. W. H. Hohne, S. T. Mixture, O. A. Graeve, *PLoS One* **2020**, *15*, e0234774.
- [57] D. Janovszky, M. Sveda, A. Sycheva, F. Kristaly, F. Zámorszky, T. Koziel, P. Bala, G. Czel, G. Kaptay, *J. Therm. Anal. Calorim.* **2022**, *147*, 7141.
- [58] E. Fazakas, B. Varga, L. K. Varga, *ISRN Metallurgy* **2012**, *5*, 602108.
- [59] C. Nunes, A. Mahendrasingam, R. Suryanarayanan, *Pharm. Res.* **2005**, *22*, 1942.
- [60] M. G. Abiad, M. T. Carvajal, O. H. Campanella, *Food Eng. Rev.* **2009**, *1*, 105.
- [61] P. Kathiravan, T. Balakrishnan, C. Srinath, K. Ramamurthi, S. Thamocharan, *KIJOMS* **2016**, *2*, 226.
- [62] R. Trejo-Tzab, L. Caballero-Espada, P. Quintana, A. Ávila-Ortega, R. A. Medina-Esquivel, *Nanoscale Res. Lett.* **2017**, *12*, 32.
- [63] G. Zhang, M. Wen, S. Wang, J. Chen, J. Wang, *RSC Adv.* **2018**, *8*, 567.
- [64] S. Li, Q. Xu, E. Uchaker, X. i Cao, G. Cao, *CrystEngComm* **2016**, *18*, 2532.
- [65] A. Sivakumar, L. Dai, S. Sahaya Jude Dhas, T. Vasanthi, V. N. Vijayakumar, S. A. Martin Britto Dhas, Communicated elsewhere **2023**.
- [66] A. Sivakumar, M. Manivannan, S. Sahaya Jude Dhas, J. Kalyana Sundar, M. Jose, S. A. Martin Britto Dhas, *Mater. Res. Express* **2019**, *6*, 086303.
- [67] A. Sivakumar, P. Eniya, S. Sahaya Jude Dhas, S. J. Dhas, J. K. Sundar, S. Stephen Rajkumar Inbanathan, M. Jose, S. A. Martin Britto Dhas, *Solid State Commun.* **2022**, *342*, 114625.
- [68] A. Sivakumar, A. Saranraj, S. S. J. Dhas, A. I. Almansour, R. S. Kumar, N. Arumugam, K. Perumal, S. A. Martin Britto Dhas, *J. Phys. Chem. C* **2021**, *125*, 25217.
- [69] A. Sivakumar, P. Eniya, S. S. J. Dhas, R. S. Kumar, A. I. Almansour, K. Sivashanmugam, J. K. Sundar, S. A. Martin Britto Dhas, *CrystEngComm* **2022**, *24*, 52.